

Circle-shaped Transformation Cavity via Center-Shift Möbius Transformation

Jinhang Cho, Inbo Kim, Sunghwan Rim, and Muhan Choi*

Digital Technology Research Center, Kyungpook National University, Daegu 41566, Republic of Korea

Yong-Hun Lee

School of Electronics Engineering, Kyungpook National University, Daegu 41566, Republic of Korea

Jung-Wan Ryu

Center for Theoretical Physics of Complex Systems,
Institute for Basic Science (IBS), Daejeon 34126, Republic of Korea

Circle-shaped transformation cavities of shifted center are the most simple transformation cavities in the sense that they have only spatial index variation without boundary shape deformation. For these cavities, we analyze the characteristics of conformal whispering gallery modes according to center-shift coordinate transformation. For this study, we use an alternative scheme for designing a transformation cavity without using a shrinking parameter that is needed to satisfy total internal reflection condition. It is observed that the isotropic emission of whispering gallery modes in the uniform index circular cavity changes to the bi-directional emission of conformal whispering gallery modes as the center-shift increases. Also, using a purity factor that quantitatively measures in RV space the degree of intactness for the internal wave pattern of resonant modes in transformation cavities compared with corresponding whispering gallery mode in uniform disk cavity, we show that the conformal whispering gallery modes in the circle-shaped transformation cavity has not only directionality but also high persistence for characteristics of whispering gallery modes.

PACS numbers: xx.xx

I. INTRODUCTION

The 2-dimensional (2D) dielectric microcavities have been intensively studied over the last two decades due to the potential as ultra-small high quality resonators needed in integrated optical circuits and sensors [1–3]. One of the core subjects in the studies is the whispering gallery modes (WGMs), a very long-lived resonances trapped by the total internal reflection (TIR). The ideal WGMs in the uniform refractive index circular cavity can have very high quality-factor (Q -factor), but their isotropic emission due to the rotational symmetry are serious drawback. Many researches have been done to overcome this problem by deforming the shape of the cavity or involving the scatterers, but it also causes Q -factor degradation and undesired complex phenomena such as wave chaos [4–7] and mode interaction effects [8–14]. As a novel approach to remedy above drawback, recently proposed are transformation cavities (TCs), dielectric cavities with the gradient refractive index (GRIN) designed based on conformal transformation optics [15]. The anisotropic WGMs supported in the TCs, so-called conformal whispering gallery modes (cWGMs), provide directional tunneling emission as well as retain Q -factors of corresponding WGMs in uniform disk cavity. The TCs can be designed through various analytic functions of complex variables or the composite functions of those. Also, even if an analytic form of conformal mapping has singularities inside the cavity region or is difficult to be

found out for a given cavity shape, the numerical conformal mapping method can be used for those cases [16].

The cWGMs in generic boundary deformed TCs have the property that both effects of shape deformation and GRIN generated by conformal mapping are intermingled. Circle-shaped TCs belong to a special class TC that is ruled by only the effect of spatial refractive index variation, completely free from the deformation effect. The circle-shaped TC can be formed by the center-shift conformal mapping which can be used as an element of composite functions to achieve a realizable refractive index profile or to break mirror symmetry for a given mirror symmetric shaped TC. The investigation of the cWGM characteristics for the circle-shaped TCs is also a groundwork on the researchs for various TCs using the center-shift conformal mapping.

This paper is organized as follows. We briefly review the center-shift conformal transformation and the original method for designing TCs using a shrinking parameter to support cWGMs in Sec. II. An alternative scheme to construct the TCs without the shrinking parameter and a circle-shaped TC constructed through this scheme is presented in Sec. III. In Sec. IV, the characteristics of cWGMs in the circle-shaped TC is numerically investigated and the purity factor for measuring the intactness of cWGM is defined and discussed. Finally we give a summary in Sec. V.

* mhchoi@ee.knu.ac.kr

II. CENTER-SHIFT CONFORMAL TRANSFORMATION AND CIRCLE-SHAPED TRANSFORMATION CAVITY WITH SHRINKING PARAMETER

A. Center-Shift Conformal Transformation

A mapping that transforms a unit circle in η -plane to a center-shifted unit circle in ζ -plane is given by the following form,

$$\zeta = \frac{\eta + \delta}{1 + \delta^* \eta}, \quad |\delta| < 1, \quad (1)$$

where $\eta = u + iv$ and $\zeta = x + iy$ are complex variables in the complex planes, respectively, and δ is a complex valued parameter representing the center-shift. This mapping forms a subgroup of Möbius transformations and we will call it the center-shift conformal transformation in this paper. Since the arbitrary center-shift can be described by taking the line of shift as the u -axis ($\delta \in \mathbb{R}$), so the above mapping can be simplified as follows:

$$\zeta = f(\eta) = \frac{\eta + \delta}{1 + \delta \eta}, \quad |\delta| < 1. \quad (2)$$

By the application of the above conformal mapping, a circle with a radius of 1 in η -plane are transformed into a center-shifted circle of the same size with the rotational symmetry broken in ζ -plane as shown in Fig. 1. For reference, the inverse conformal mapping from ζ -plane to η -plane is expressed as follows:

$$\eta = g(\zeta) = \frac{\zeta - \delta}{1 - \delta \zeta}, \quad |\delta| < 1. \quad (3)$$

B. Circle-Shaped Transformation Cavity with Shrinking Parameter

Next, we look at the TCs which is previously proposed in [15]. Considering the translational symmetry

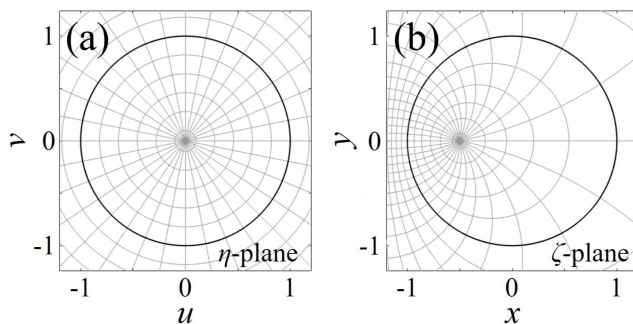


Figure 1. Conceptual diagrams for center-shift conformal transformation from (a) η -plane to (b) ζ -plane.

along the z -axis in a infinite cylindrical dielectric cavity, the Maxwell equations can be reduced to effective 2-dimensional scalar wave equation. Resonances in a TC satisfying the outgoing-wave boundary condition, $\psi(\mathbf{r}) \sim h(\phi, k)e^{ikr}/\sqrt{r}$ for $r \rightarrow \infty$, where position vector $\mathbf{r} = (x, y) = (r \cos \phi, r \sin \phi)$, k is the vacuum wavenumber, and $h(\phi, k)$ is the far-field angular distribution of the emission, are obtained as the solutions of following wave equation,

$$[\nabla^2 + n^2(\mathbf{r})k^2] \psi(\mathbf{r}) = 0, \quad (4)$$

with the refractive index $n(\mathbf{r})$ given by

$$n(\mathbf{r}) = \begin{cases} n_0 \left| \frac{d\zeta}{d\eta} \right|^{-1}, & \text{(interior)} \\ 1, & \text{(exterior)} \end{cases}. \quad (5)$$

For the transverse magnetic (TM) polarization, the wave function $\psi(\mathbf{r})$ represents E_z , the z component of electric field, and both the wave function $\psi(\mathbf{r})$ and its normal derivative $\partial_v \psi(\mathbf{r})$ are continuous across the cavity boundary. For the transverse electric (TE) polarization, the wave function $\psi(\mathbf{r})$ represents H_z , the z component of magnetic field, and both $\psi(\mathbf{r})$ and $n(\mathbf{r})^{-2} \partial_v \psi$ are continuous across the cavity boundary. By the outgoing-wave boundary condition, the resonances, which have discrete complex wavenumbers k_r with negative imaginary parts, exponentially decay in time. The frequency and the lifetime of a resonance are given by $\omega = c\text{Re}[k_r]$ and $\tau = -1/2c\text{Im}[k_r]$ where c is light speed in vacuum, respectively. The quality factor of a resonance is defined as $Q = 2\pi\tau/T = -\text{Re}[k_r]/2\text{Im}[k_r]$ where the oscillation period of light wave is $T = 2\pi/\omega$.

To describe the conventional method for constructing TCs supporting cWGMs, four spaces are usually considered : original virtual (OV), wholly transformed (WT), physical (Ph), and reciprocal virtual (RV) spaces [17]. First, a disk cavity with a homogeneous refractive index n_0 and a unit radius R_0 is considered in complex η -plane called OV space. The uniform index disk cavity in the OV space is conformally transformed to a cavity in complex ζ -plane called WT space through a entire spatial conformal mapping multiplied by β , such as a resizable center-shift transformation,

$$\zeta = \beta f(\eta) = \beta \frac{\eta + \delta}{1 + \delta \eta}, \quad |\delta| < 1. \quad (6)$$

In the WT space, interior and exterior refractive index profiles of the cavity are inhomogeneous but the relative refractive index at the boundary interface remains homogeneous, because the two cavities in OV and WT spaces are mathematically equivalent. Next, we set the exterior GRIN profile in WT space to 1 considering the realistic physical situation then, finally, we can obtain a circle-shaped TC in physical space. The refractive index of the

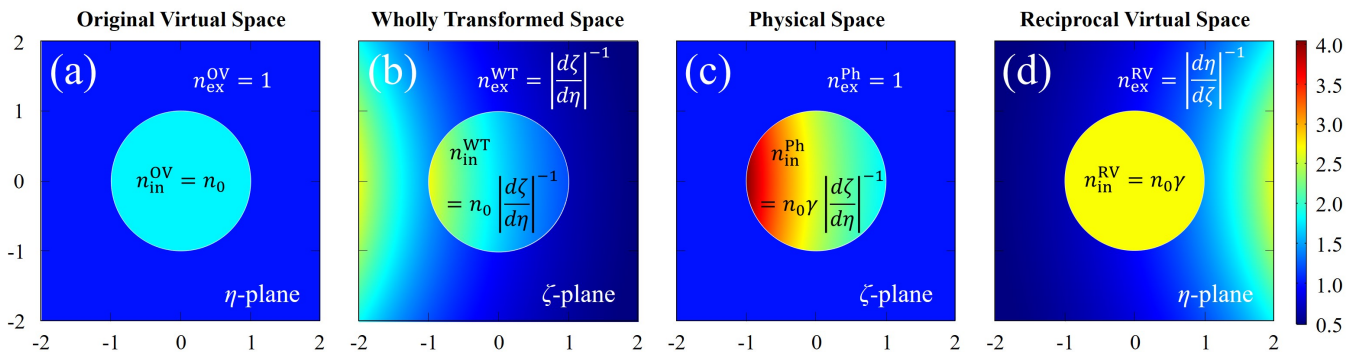


Figure 2. Refractive index profiles in (a) original virtual, (b) wholly transformed, (c) physical, and (d) reciprocal virtual spaces. These pictures were drawn in circle-shaped transformation cavity without a shrinking parameter at $n_0 = 1.8$, $|\delta| = 0.2$, and $\gamma = \gamma_{\min}$.

circle-shaped TC in physical space can be derived from Eq. (6) as following form,

$$n(\mathbf{r}) = \begin{cases} n_0 \left| \frac{(\beta - \delta\zeta)^2}{\beta(\delta^2 - 1)} \right|^{-1}, & |\delta| < 1, \quad (\text{interior}) \\ 1, & (\text{exterior}) \end{cases}. \quad (7)$$

The relative refractive index at the boundary interface is not homogeneous in the physical space. The heterogeneity of the relative refractive index acts as an important factor in forming the resonance characteristics which differ from in a uniform index disk cavity, and the reason can be easily predicted through RV space which is mathematically equivalent to the physical space. The RV space can be obtained from inverse conformal transformation over the entire domain of physical space.

In order to obtain cWGMs in the TCs, we finally apply a specific value β_{\max} or lower to β such that the minimum value of the internal refractive index profile is at least n_0 . This is a TIR minimum condition that reduces the size of the cavity and at the same time allows the ray trajectory at the boundary to satisfy the TIR angle. The TIR minimum condition in this case is obtained as follows:

$$\beta_{\max} \equiv \frac{1 - |\delta|}{1 + |\delta|}, \quad |\delta| < 1. \quad (8)$$

Here, we note that $|d\zeta/d\eta|^{-1}$ which forms the refractive index of TCs, is a function of β , so not only the cavity size but the GRIN profile changes according to the change of β .

III. CIRCLE-SHAPED TRANSFORMATION CAVITY WITHOUT SHRINKING PARAMETER

In the aforementioned constructing method, the cavity maintains the unit size in the RV space, but not in

the physical space because of the shrinking parameter. In particular, for the case of a circle-shaped TC with no boundary shape change, it is easier to analyze pure spatial index variation to completely exclude the parametrically changed variables related to the boundary. Here, we propose a new TC design scheme that maintains the dimensionless coordinates [1] in physical space by eliminating the size-scaling by conformal mapping. We first consider a uniform index disk cavity in OV space (η -plane) with the unit radius R_0 and the invariant reference refractive index n_0 and then, conformally transform the entire space multiplied by an index-proportion parameter γ into a WT space (ζ -plane) through the mapping equation without β , Eq. (2). Finally, forcing the exterior refractive index to 1 yields the TC in physical space. As a result, the interior and exterior refractive index in the physical space is as follows:

$$n(\mathbf{r}) = \begin{cases} n_{\text{in}}^{\text{Ph}} = n_0 \gamma \left| \frac{d\zeta}{d\eta} \right|^{-1}, & (\text{interior}) \\ n_{\text{ex}}^{\text{Ph}} = 1, & (\text{exterior}) \end{cases}. \quad (9)$$

Additionally, through the inverse transformation from ζ -plane to η -plane, the interior and exterior refractive index in RV space can be obtained as follows:

$$\tilde{n}(\tilde{\mathbf{r}}) = \begin{cases} n_{\text{in}}^{\text{RV}} = n_0 \gamma, & (\text{interior}) \\ n_{\text{ex}}^{\text{RV}} = \left| \frac{d\eta}{d\zeta} \right|^{-1}, & (\text{exterior}) \end{cases}. \quad (10)$$

where position vector $\tilde{\mathbf{r}} = (u, v)$. We shortly call this newly constructed TC to γ -type TC and, for clarity, we refer to the conventional TC as the β -type TC. γ -type TC can satisfy the TIR condition by increasing the interior refractive index in physical space independently of the profile-generating factor, $|d\zeta/d\eta|^{-1}$ of Eq. (9), without reducing the cavity size. This is the most noticeable difference from the β -type TC, in which decreasing β reduces the cavity size and simultaneously increases the profile-generating factor of Eq. (5) as a whole. To help

understand, we have drawn conceptual diagrams of four spaces using in the γ -type circle-shaped TC in Fig. 2.

β -type and γ -type are perfectly identical systems in the viewpoint of physics. In the case of γ -type, k_r means the dimensionless resonant wavenumber and multiplying k_r by $n_0\gamma$ changed by TIR condition gives the internal dimensionless resonant wavenumber, $\kappa \equiv n_0\gamma k_r R_0$. The free-space wavenumber in β -type is obtained by dividing k_r in γ -type by β . One can properly select and use at convenience among the two types. γ -type can be more advantageous in terms of theoretical and numerical study such as analyzing the changes of resonance distribution in a given wavelength region, adjusting the target frequency of the resonance to be observed, tracing a specific resonance to finding the optimizing conditions, or reobtaining the refractive index profile for designing on real fabrication.

	β -type TC	γ -type TC
conformal transformation	$\zeta = \beta f(\eta)$	$\zeta = f(\eta)$
refractive index in RV space	$n_{\text{in}}^{\text{RV}} = n_0$	$n_{\text{in}}^{\text{RV}} = n_0\gamma$
radius of cavity in physical space	$\beta R_0 = \beta$	$R_0 = 1$
refractive index in physical space	$n_{\text{in}}^{\text{Ph}} = n(\zeta, \beta)$	$n_{\text{in}}^{\text{Ph}} = n(\zeta)\gamma$

Table I. Comparison between β -type and γ -type TCs

By the center-shift conformal transformation Eq. (2), the disk cavity with homogeneous interior refractive index n_0 in OV space is transformed to the γ -type circle-shaped TC with the following inhomogeneous interior refractive index profile in the physical space.

$$n_{\text{in}}^{\text{Ph}}(\zeta) = n_0\gamma \left| \frac{(1 - \delta\zeta)^2}{(\delta^2 - 1)} \right|^{-1}, \quad |\delta| < 1, \quad (11)$$

Also, we can derive the profile of exterior refractive index for γ -type TC in the RV space through the inverse conformal mapping Eq. (3) as follows:

$$n_{\text{ex}}^{\text{RV}}(\eta) = \left| \frac{(1 - \delta^2)}{(1 + \delta\eta)^2} \right|, \quad |\delta| < 1. \quad (12)$$

To obtain cWGMs formed by TIR, the condition is required that the minimum value of the interior refractive index profile is at least greater than n_0 and we define γ satisfying this condition as γ_{min} . In the case of γ -type circle-shaped TC, $n_{\text{in}}^{\text{Ph}}$ has the minimum value at $\eta = -\delta/|\delta|$, thus γ_{min} is given as follows:

$$\gamma_{\text{min}} \equiv \frac{1 + |\delta|}{1 - |\delta|}, \quad |\delta| < 1. \quad (13)$$

Comparing the above equation with Eq. (8) used in β -type TC, we can see that γ_{min} lies in the relationship of $1/\beta_{\text{max}}$.

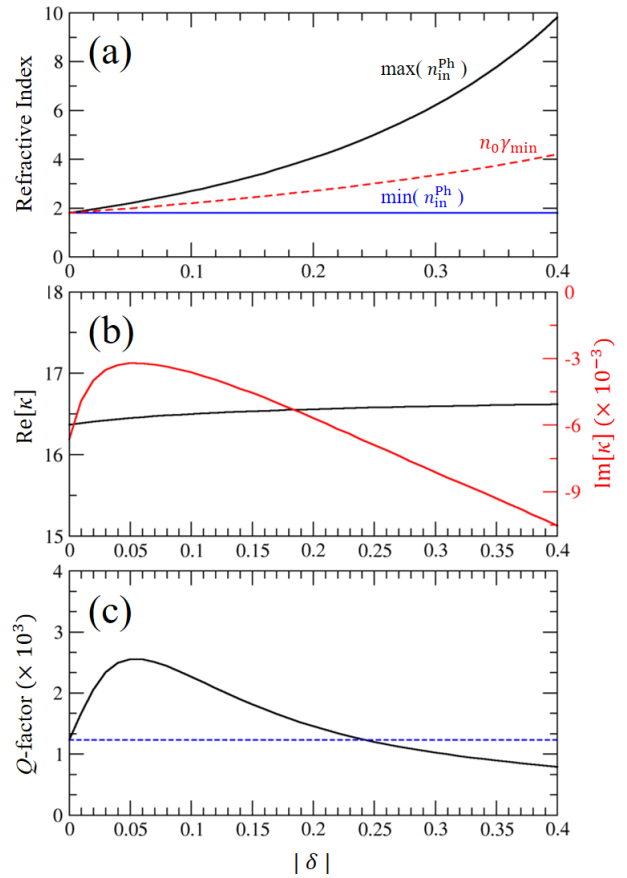


Figure 3. (a) is the changes of the range of refractive index profile $n_{\text{in}}^{\text{Ph}}$ (black and blue solid line) and the value of $n_0\gamma_{\text{min}}$ (red dashed line) according to the center-shift parameters $|\delta|$ in the γ -type circle-shaped TC with $n_0 = 1.8$ and $\gamma = \gamma_{\text{min}}$. (b) and (c) are the changes of internal dimensionless wavenumber κ and Q -factor for M(13,1) that varies with $|\delta|$, respectively. Black and red lines in (b) are the real and the imaginary parts of $\kappa = n_0\gamma k_r R_0$, respectively. Blue dashed lines in (c) are Q -factor in the uniform index disk cavity with n_0 .

IV. NUMERICAL RESULTS

A. cWGMs in Circle-Shaped Transformation Cavity

Using the γ -type circle-shaped TC presented above, we investigate the characteristic changes of a specific cWGM for TM polarization by changing in the range of $0 \leq |\delta| \leq 0.4$ under the fixed conditions of reference refractive index $n_0 = 1.8$ and index-proportion parameter $\gamma = \gamma_{\text{min}}$. These results can be obtained from either finite element method (FEM) or boundary element method (BEM) [17], FEM-based COMSOL Multiphysics were used in this study. Also, in this paper, we assign cWGMs to M(m, l) as a combination of mode indices corresponding to the angular momentum index m and the radial nodal number l in the uniform index disk cavity. According to the change of $|\delta|$, the interior refractive

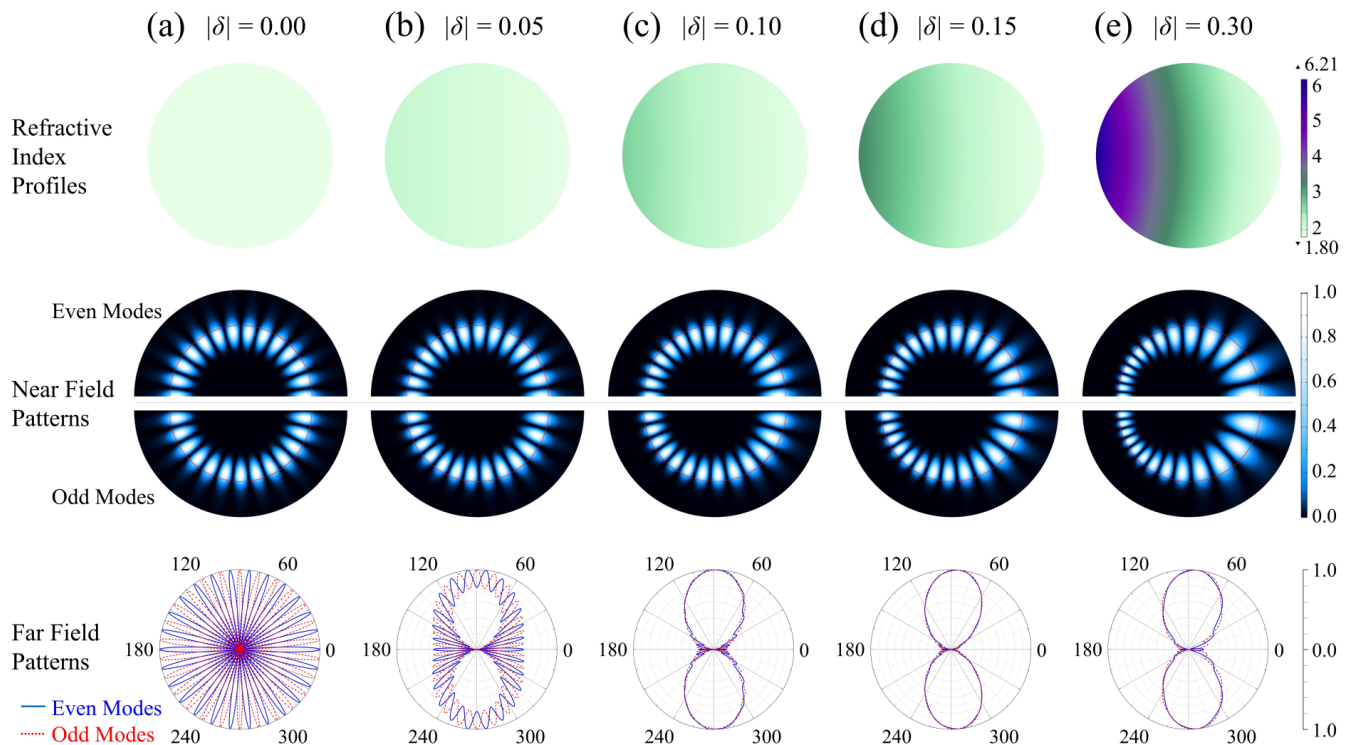


Figure 4. Refractive index profile and near field and far field intensity patterns for the mode pair of $M(13,1)$ at the shifting parameter (a) $|\delta| = 0$, (b) 0.05, (c) 0.10, (d) 0.15, and (e) 0.30 in the γ -type circle-shaped TC with $n_0 = 1.8$ and $\gamma = \gamma_{\min}$. The refractive index of outside cavity set to air. In each step, up-side (down-side) of near field pattern and blue solid (red dashed) line in far-field pattern are the even-parity (odd-parity) mode.

index in OV space and the maximum and minimum value of interior refractive index profile in physical spaces are changed as shown in Fig. 3 (a). As $|\delta|$ increases, the maximum value of refractive index profile $n_{\text{in}}^{\text{Ph}}$ gradually widens the overall variation of the index profile with n_0 as the baseline. At the same time, γ_{\min} also increases to satisfy the TIR condition as shown in Fig. 3 (b).

The internal dimensionless wavenumbers χ and Q -factors for the mode pair of $M(13,1)$ are changed as shown in Fig. 3 (c) and (d), respectively. In the uniform index disk cavity case with $|\delta| = 0$, all resonances except for the case with $m = 0$ are in doubly degenerate states due to the rotational symmetry. Each degenerate pair is nearly degenerate under the condition of $|\delta| > 0$ and each nearly degenerate pair can be divided into even- and odd-parity modes due to the mirror symmetry for the x -axis. Nevertheless, in the range we show, the wavelength values for the cWGM pair appear to overlap almost one with no significant deviation. In terms of the RV space shown in Fig. 2 (d)), it means that the cWGM pair is very little affected by the pure change in relative refractive index at the boundary interface caused by $|\delta|$ in our range.

As shown in Fig. 3 (c), $\text{Re}[\kappa]$ associated with the internal wavelength of the mode pair of $M(13,1)$ does not change significantly with the varying in $|\delta|$, on the other hand, $\text{Im}[\kappa]$ grows larger than that in the homogeneous

case and then decreases from a certain threshold (in our case, about $|\delta| = 0.05$) as $|\delta|$ increases. It is directly reflected in the Q -factor in Fig. 3 (d). The temporary rise of Q -factor, which is typical aspect of cWGMs in TC satisfying the TIR condition [15, 19], is caused by the overall increasement in the refractive index profile of TC due to the TIR condition, and the increment of γ_{\min} in the γ -type TC well explains why such behavior occurs.

For the case of $|\delta| \neq 0$, the relative refractive index at the boundary interface and the interior refractive index profile exhibit a dipole distribution similar to the case of the limaçon TC [15]. Considering the emitting mechanism described through the Husimi function [18], cWGMs in the circle-shaped TC can be predicted to have a similar mode properties. We show the stepwise change of refractive index profile and near- and far-field intensity patterns for a even-odd mode pair of $M(13,1)$ at $|\delta| = 0, 0.05, 0.10, 0.15,$ and 0.30 in Fig. 4. As $|\delta|$ increases, the dipole distribution of the refractive index becomes more pronounced due to the increase in the variation width of the index profile, while the near field intensity pattern at all steps maintains a cWGM morphology confined well along the boundary.

In Ref. [18, 19], it has already discussed that the emission of cWGMs satisfying the TIR condition is tunneled out as an evanescent wave in the region where the refrac-

tive index is relatively low and, as the deformation parameter increases, the nearly flat intensity band structure on the Husimi function for cWGMs is almost unchanged, while the shape of the critical line is further bent by the variation of the relative refractive index at the boundary interface. Such non-constant critical angle creates a unique light emission mechanism which the light tunnels out at regions where the band structure is relatively close to the critical angle. i.e., where the relative refractive index at the boundary interface is relatively low.

In the TCs with a dipole distributed refractive index profile, the critical line approaches the band structure only in one place, which creates a single point emitting mechanism, and their external waves form bi-directional emission if they have an axis symmetry. We can confirm it through the far field intensity patterns in Fig. 4. As $|\delta|$ increases, the isotropic emission of mode pair when $|\delta| = 0$ turns into the bi-directional emission and the mode pairs in each step have the same tendency for the far-field intensity distribution regardless of parity. The bi-directionality is bestly improved at $|\delta| = 0.15$. Incidentally, if $|\delta| \geq 0.2$, the maximum value of refractive index profile requires a large rise above 4 which is difficult to implement, but the far field distribution still has bi-directionality.

B. Purity Factor for cWGMs

We are here to present another tool for characterizing cWGMs. RV space is easier to analyze the mode characteristics since it is the equivalent space with physical space and formed with unit disk cavity with uniform refractive index. In general, when the uniform index disk cavity is progressively distorted by the shape deformation, WGMs with perfect rotational symmetry begin to lose their inherent properties, accompanied by the Q -spoiling and the pattern distortion by the synthesis of several angular momentum components. The angular momentum decomposition is very useful method for analyzing such the angular momentum distribution [20]. The spread of m derived from the analysis of angular momentum components for a resonant mode can be used to gauge how much the resonance in a slightly deformed cavity is distorted from a specific resonance in the uniform index disk cavity. Such distortion also occurs at the resonances in TCs. In the case of homogeneous cavities, the distortion is due to the effect of shape deformation, whereas in the case of circle-shaped TC without shape deformation, it is caused by the non-uniformity of the relative refractive index at the boundary interface. The variation of the distortion rate for each mode according to the change of the system parameters has different criteria according to the lifetime and wavelength of the resonance, but it is sufficient to check how long the WGM characteristics of the uniform index disk cavity are maintained in the cWGM.

To analyze the inherent mode properties inside TCs, we introduce the angular momentum distribution in RV

space equivalent with physical space. In RV space, the wave function inside the uniform index disk cavity can be expanded to cylindrical harmonics in polar coordinates as follows:

$$\psi(r_{\text{RV}}, \phi_{\text{RV}}) = \sum_{m=-\infty}^{\infty} \alpha_m J_m \left(\kappa \frac{r_{\text{RV}}}{R_0} \right) e^{im\phi_{\text{RV}}}, \quad (14)$$

where $r_{\text{RV}} (< R_0)$ and ϕ_{RV} are the radius and angle of the position on the data pickup domain, respectively, $+$ ($-$) signs of angular momentum index mean CCW (CW) traveling-wave components, α_m is the angular momentum distribution for m , and J_m is the m th-order Bessel function of the first kind. α_m is obtained through the Fourier expansion of the above equation. Note that the data pickup domain must be chosen as a concentric circle with a center of mass in the RV space, taking into account the spatial transformation by conformal mapping. From the above angular momentum distribution, our newly proposed measurand that estimates the mode distortion rate, namely purity factor, can be simply defined as follows :

$$P = \frac{|\alpha_d|^2}{\sum_{m=0}^{\infty} |\alpha_m|^2}, \quad (15)$$

where α_d is that for a dominant angular momentum index d . Under the our situation of standing wave conditions by axis symmetry, we only need to take one component, CCW or CW. This P -factor means the contribution of resonance with $m = d$ in the uniform index disk cavity in forming a specific resonance we are going to observe in TCs.

To investigating the change of distortion rate for the cWGM, we obtained the above P -factor for M(13,1) in the range of $0 \leq |\delta| \leq 0.4$ where the data pickup domain $r_{\text{RV}} = 0.8$. We plotted it in Fig. 5 attaching the P -factor for M(13,2) for comparison. The $|\delta|$ -dependent increase in the heterogeneity of the relative refractive index at the boundary interface, which acts as an effective deformation effect, reduces overall the P -factor for both modes. Here, it should be noted that the variation of the P -factor for M(13,1) is very small. It means that the resonance properties in the uniform index disk cavity are maintained fairly well in cWGMs with $l = 1$. Whereas M(13,2), which relatively less satisfies the TIR condition, reacts more sensitively to the center-shift parametric changes on the boundary relative refractive index variation, resulting in a greater collapse of the P -factor.

V. SUMMARY

In this paper, we have newly proposed a construction scheme for TC without the shrinking parameter related to TIR condition, and, in the circle-shaped TC using

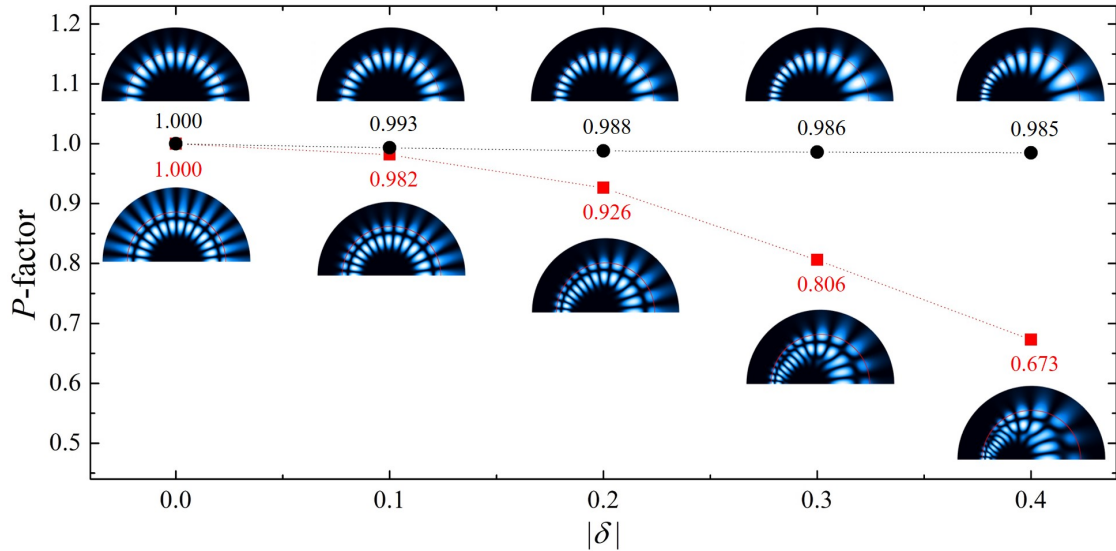


Figure 5. The change of P -factors for even-parity modes of (a) M(13,1) and (b) M(13,2) according to $|\delta|$ in γ -type circle-shaped TC with $n_0 = 1.8$ and $\gamma = \gamma_{\min}$. The data pickup domain for P -factors is set to $r_{\text{RV}} = 0.8$ and the intensity of the near field patterns is normalized linear scale.

it, investigated the characteristic changes of a cWGM of which isotropic emission breaks in bi-directional emission as the center-shift parameter increases. The enhancement of distortion effect on the modes due to the pure spatial refractive index variation according to the center-shift parameter can be verified through the newly defined purity factor P indicating how much the nature of WGM in the uniform index disk cavity is maintained via the angular momentum distribution in the RV space. In conclusion, it has been examined that the circle-shaped TC can produce the bi-directional emitting fundamental cWGMs of which P -factor is nearly one.

ACKNOWLEDGMENTS

We would like to thank Y. Kim and S.-J. Park for helpful discussions. This work was supported by the National Research Foundation of Korea (NRF) grant funded by the Korean government (MSIP) (2017R1A2B4012045 and 2017R1A4A1015565) and the Institute for Basic Science of Korea (IBS-R024-D1).

-
- [1] Chang, R. K., and A. J. Campillo, *Optical Processes in Microcavities* (World Scientific, Singapore, 1996).
 - [2] K. J. Vahala, "Optical microcavities," *Nature* **424**, 839 (2003).
 - [3] H. Cao and J. Wiersig, "Dielectric microcavities: Model systems for wave chaos and non-Hermitian physics," *Rev. Mod. Phys.* **87**, 61 (2015).
 - [4] J. U. Nöckel and A. D. Stone, "Ray and wave chaos in asymmetric resonant optical cavities," *Nature* **385**, 45 (1997).
 - [5] S.-B. Lee, J.-H. Lee, J.-S. Chang, H.-J. Moon, S. W. Kim, and K. An, "Observation of Scarred Modes in Asymmetrically Deformed Microcylinder Lasers," *Phys. Rev. Lett.* **88**, 033903 (2002).
 - [6] S. Shinohara, T. Harayama, T. Fukushima, M. Hentschel, T. Sasaki, and E. E. Narimanov, "Chaos-Assisted Directional Light Emission from Microcavity Lasers," *Phys. Rev. Lett.* **104**, 163902 (2010).
 - [7] S. Sunada, S. Shinohara, T. Fukushima, and T. Harayama, "Signature of Wave Chaos in Spectral Characteristics of Microcavity Lasers," *Phys. Rev. Lett.* **116**, 203903 (2016).
 - [8] W. D. Heiss, "Repulsion of resonance states and exceptional points," *Phys. Rev. E* **61**, 929 (2000).
 - [9] J. Wiersig, "Formation of Long-Lived, Scarlike Modes near Avoided Resonance Crossings in Optical Microcavities," *Phys. Rev. Lett.* **97**, 253901 (2006).
 - [10] J. Wiersig and M. Hentschel, "Unidirectional light emission from high-Q modes in optical microcavities," *Phys. Rev. A* **73**, 031802(R) (2006).
 - [11] S.-Y. Lee, J.-W. Ryu, J.-B. Shim, S.-B. Lee, S. W. Kim, and K. An, "Divergent Petermann factor of interacting resonances in a stadium-shaped microcavity," *Phys. Rev. A* **78**, 015805 (2008).
 - [12] J. Wiersig, S. W. Kim, and M. Hentschel, "Asymmetric scattering and nonorthogonal mode patterns in optical microspirals," *Phys. Rev. A* **78**, 053809 (2008).
 - [13] J.-W. Ryu, S.-Y. Lee, and S. W. Kim, "Coupled non-identical microdisks: Avoided crossing of energy levels and unidirectional far-field emission," *Phys. Rev. A* **79**,

- 053858 (2009).
- [14] C.-W. Yi, J. Kullig, and J. Wiersig, "Pair of Exceptional Points in a Microdisk Cavity under an Extremely Weak Deformation," *Phys. Rev. Lett.* **120**, 093902 (2018).
 - [15] Y. Kim, S. H. Lee, J. W. Ryu, I. Kim, J. H. Han, H. S. Tae, M. Choi, and B. Min, "Designing whispering gallery modes via transformation optics," *Nature Photonics* **10**, 647 (2016).
 - [16] S.-J. Park, I. Kim, J. Cho, Y. Kim, and M. Choi, "Designing arbitrary-shaped whispering-gallery cavities based on transformation optics," *Opt. Express* **27**, 16320-16328 (2019).
 - [17] J.-W. Ryu, J. Cho, S.-Y. Lee, Y. Kim, S.-J. Park, S. Rim, M. Choi, and I. Kim, "Boundary integral equation method for resonances in gradient index cavities designed by conformal transformation optics" *Scientific Reports* **9**, 19684 (2019).
 - [18] I. Kim, J. Cho, Y. Kim, B. Min, J.-W. Ryu, S. Rim, and M. Choi, "Husimi functions at gradient index cavities designed by conformal transformation optics," *Opt. Express* **26**, 6851-6859 (2018).
 - [19] J.-W. Ryu, J. Cho, I. Kim, and M. Choi, "Optimization of conformal whispering gallery modes in limaçon-shaped transformation cavities," *Scientific Reports* **9**, 8506 (2019).
 - [20] J. Wiersig, S. W. Kim, and M. Hentschel, "Asymmetric scattering and nonorthogonal mode patterns in optical microspirals," *Phys. Rev. A* **78**, 053809 (2008).